Ozonesonde Launches in 2023

Final Report

Grant Number: 582-18-81339
Proposal for Grant Activities No. 582-23-41323-026
Tracking No. 2023-12

Prepared for the Texas Commission on Environmental Quality (TCEQ)

Principal Investigators:

James Flynn, *University of Houston*

Paul Walter, *St. Edward's University*

Thomas Gill, *University of Texas at El Paso*

Kristina Trevino, *Trinity University*

Prepared by:

Paul Walter

March 14, 2024

Executive Summary

During the period 26 May – 17 October 2023, a team of researchers from the University of Houston, St. Edward's University, Trinity University, and the University of Texas at El Paso carried out a total of 60 ozonesonde launches in El Paso, San Antonio, and Houston, Texas (26 launches from El Paso, 24 from San Antonio, and 10 launches from Houston). This effort had the primary purpose to sample, characterize, and explain ozone and meteorological features in the boundary layer, the lower free troposphere (LFT), and the upper troposphere/lower stratosphere (UTLS) in these regions. Launches were targeted at days when ozone was expected to exceed the level of the Federal standard to inform and improve our understanding of conditions under which such exceedances could occur. The data collected from San Antonio and El Paso builds on past ozonesonde campaigns in 2017, 2019, and 2020. The data collected from Houston builds upon the 2021 TRacking Aerosol Convection ExpeRiment – Air Quality (TRACER-AQ) and 2022 TRACER-AQ2 campaigns (Jensen et al., 2022; Judd et al., 2021). Data from this project support analyses of conditions associated with high ozone events in these regions.

During the sampling period, there were seven days where the max daily 8-hour average (MDA) ozone concentration for the El Paso region exceeded the 2015 National Ambient Air Quality Standard (NAAQS) of MDA8 [O3] ≤ 70 ppbv. The Continuous Ambient Monitoring Station (CAMS) C1021 Ojo de Agua site located in northwestern El Paso to the west of the Franklin mountains recorded ozone exceedance events on all seven of those days and on all but one day was the highest monitor the region.

For the 2023 San Antonio campaign, there were two days in August and four days in September that exceeded the NAAQS ozone standard and had ozonesonde launches. The days exceeding the ozone standard were during post-frontal conditions. The monitor recording the highest ozone was on the northwest side of San Antonio for three of those six days, and such days showed light winds in the morning shifting to out of the SE in the afternoon. The profiles of the dawn flights showed that background ozone leftover in the residual layer from the previous day significantly contributed to the higher ozone days in San Antonio. For days that did not exceed the ozone standard, consistent southerly flow regularly brought relatively clean marine air and strong winds to San Antonio.

Ten ozonesondes for this project were launched from the Houston-Galveston-Brazoria region in September 2023. Four days with ozonesonde launches had a monitor exceed the ozone standard, and those events spanned a range of conditions. Two of the exceedance days showed effects from a sea breeze leading to a flow reversal followed by increases in ozone concentrations.

Table of Contents

Table of Figures

Table of Tables

List of Abbreviations

CAMS	Continuous Ambient Monitoring Station
EPA	Environmental Protection Agency
HGB	Houston-Galveston-Brazoria
LT	local time
MDA8	maximum daily 8-hour average
NAAQS	National Ambient Air Quality Standard
RH	relative humidity
SEU	St. Edward’s University
TCEQ	Texas Commission on Environmental Quality
TU	Trinity University
UH	University of Houston
UTC	Coordinated Universal Time
UTEP	University of Texas at El Paso
Z	Zulu time (same as UTC)

1. Introduction

Ozonesondes have been launched from weather balloons in Texas since 2004. Two components of the payload make measurements: the ozonesonde, which measures ozone, and the radiosonde, which measures pressure, temperature, humidity, latitude, longitude, altitude, wind speed, and wind direction (with the last five in the list coming from an integrated GPS instrument). Connected to the ozonesonde, the radiosonde transmits a packet of data every second in the reserved FM radio band for meteorological instruments to researchers at the surface using an antenna and a receiver, who collect the data with an antenna attached to a receiver and a computer with software to decode the signal. As a result, researchers do not need to recover the ozonesonde after the flight to obtain the data. Hereafter, we will refer to the entire payload as an ozonesonde.

Ozonesondes rise at ~5 m/s and make it to altitudes of ~24 km or ~30 km depending on the size of the balloon we use. A key advantage of ozonesondes is that they augment two-dimensional surface observations by providing a vertical component, a profile of ozone and meteorology, resulting in a three-dimensional snapshot of the ozone concentration throughout the troposphere and into the stratosphere. The surface monitoring network can provide an estimate of background transported ozone but is not able to measure ozone aloft that may mix down into the boundary layer, influencing daily ozone maxima. Furthermore, information from ozonesondes allows researchers to determine the boundary layer height, a key element that influences surface pollution concentrations in both the real and modeled atmosphere.

In Section 1.1 we will examine how ozonesonde data can be used to identify the long-range transport of ozone that contributes to the observed ozone concentrations in the boundary layer. In so doing, we will discuss how to identify potential contributions from biomass burning influences and to identify potential stratospheric air that has made its way into the troposphere.

In Section 1.2 we demonstrate how ozonesonde flights at dawn provide information about ozone concentrations in both the nocturnal boundary layer (at the surface) as well as the residual layer (aloft, but at an altitude that can be entrained in the growing morning boundary layer). Both layers can influence ozone concentrations near the surface and in the afternoon boundary layer.

In Sections 2 and 3, we review the field campaigns in El Paso and San Antonio, respectively. In Section 4, we review the ozonesonde measurements from Houston. In Section 5 we provide conclusions.

In 2023, a total of 60 ozonesondes were launched from El Paso, San Antonio, and Houston (26 from El Paso, 24 from San Antonio, and 10 from Houston). The data for this project is available on the NASA STAQS data archive: https://www-air.larc.nasa.gov/cgi-bin/ArcView/staqs?SONDE=1. All flight times in this report are Coordinated Universal Time (UTC or Z). Note that 21Z is the same as 21:00 UTC. UTC is 6 hours ahead of Central

Standard Time (local San Antonio and Houston standard time), and 7 hours ahead of Mountain Standard Time (local El Paso standard time).

1.1. Identifying Long-range Transport

Signs of long-range transport of ozone that can contribute to the boundary layer can be identified through analysis of ozonesonde profiles. Such cases of long-range transport are often the result of either stratosphere-troposphere exchange (STE) or influences of biomass burning.

In an effort to better understand the factors controlling vertical O3 distribution, we examine the difference in O3 between the 1-km layer in the lower free troposphere (LFT) immediately above the mixed layer (ML) and the O3 in the ML. **Figure 1** shows an example profile identifying these two layers from a flight that occurred from Houston. The mixed layer height is determined by examining gradients in relative humidity (RH), O3, temperature, and potential temperature (θ) and is identified as the height at which most (if not all) of these variables show a sharp vertical gradient. Furthermore, we define three cases based on the RH and O3 found in the 1-km layer in the LFT: Case 1 finds a maximum O3 < 70 ppb with a minimum RH < 10%; Case 2 finds a maximum O3 > 70 ppb with a minimum RH > 40%; and Case 3 finds a maximum O3 > 70 ppb and a minimum RH < 10%. Case 1 potentially suggests UT/LS air has been transported to the LFT which may be high in O3, but not high enough on its own to trigger a violation of the EPA 8-hour O3 standard. Case 2 is potentially indicative of high O3 air that likely has an anthropogenic or biomass burning source. The high RH values associated with the high O3 suggest sources near the surface or in the lower troposphere. The O3 concentrations exceed the EPA 8-hour O3 standard. On these occasions, local violations may occur with contributions from transported O3. Finally, Case 3 is potentially indicative of high O3 air descending from the UT/LS to the LFT, low enough where it may interact with the ML or residual layer (RL) air masses. Since the O3 concentration in this LFT layer exceeds the EPA 8-hour O3 standard, these are cases in which violations may occur with contributions from naturally produced and transported stratospheric O3. For each of the cases, support for the interpretations of the observed vertical ozone distributions can be strengthened by performing HYSPLIT back trajectories to determine where the air parcels were transported from, comparing to other available chemical measurements, and other nearby soundings of radiosondes, if available.

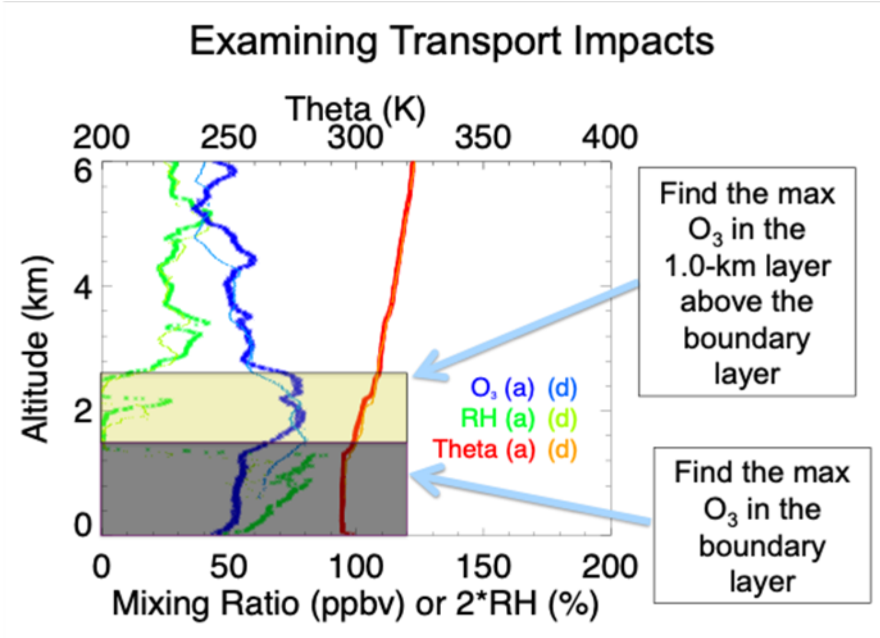

Figure 1. *The figure shows an example profile used to determine O3 in the lower free troposphere (LFT) and the mixed layer (ML). ML height determinations are made using O3, RH, temperature (not shown), and potential temperature (θ) data. See text for details. The thick lines are data of the ascent of the ozonesonde and the thin lines show the descent. Our focus will typically be on the ascending data.*

The image on the left in Figure 2 shows the profile from the first flight of the 2017 campaign from El Paso. The top of the boundary layer is specified by the black horizontal line. Higher ozone above the boundary layer suggests ozone has been transported into the area. Much more common is the situation we see in the image on the right in Figure 2 where the ozone gradient is negative (the ozone concentration decreases) just above the boundary layer. This pattern suggests the highest ozone has formed locally in the boundary layer instead of being transported into the area. Once an ozone enhancement associated with long-range transport is identified, as with the afternoon flight on 15 May 2017, further investigations are needed to identify potential upwind sources.

In most cases, the top of the boundary layer is straightforward to identify for afternoon profiles. The afternoon boundary layer is well mixed and thus the ozone concentration is relatively uniform throughout (somewhat lower concentrations near the surface due to deposition and/or titration of ozone by fresh NO emissions). At the top of the afternoon boundary layer, there are simultaneously sharp gradients (i.e., kinks) in the relative humidity, ozone concentration, and potential temperature.

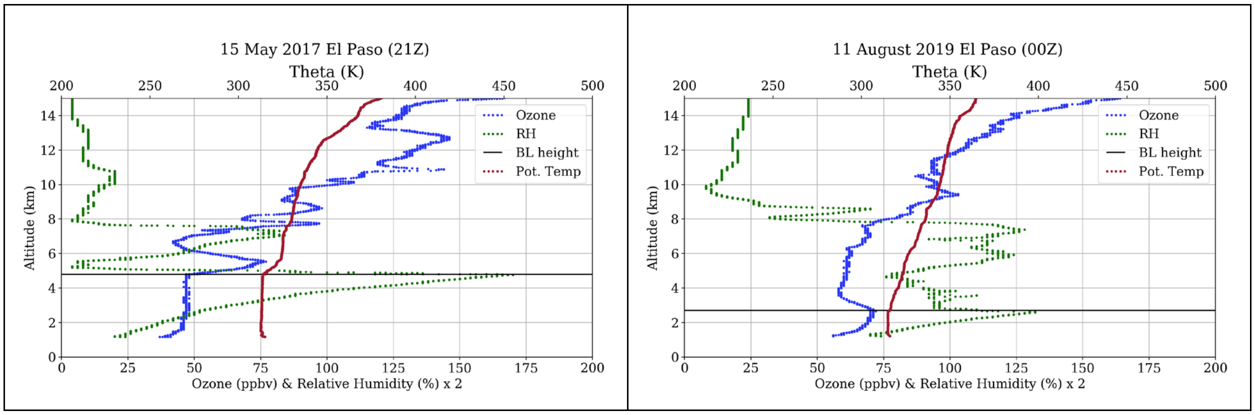

Figure 2. *Left: Just above the boundary layer there is a positive gradient in the ozone concentration (it increases), which is a sign of long-range transport. Right: Just above the boundary layer there is a negative gradient in the ozone concentration (it decreases), which is more common, meaning long-range transport is less likely and that the ozone in the boundary layer is more likely the result of local photochemical production, local transport, and contributions from the nocturnal boundary layer of the previous night.*

1.1.1. Potential Influences due to Biomass Burning

Ozone enhancements, like the one just above the boundary layer on the left image in Figure 2, can potentially be the result influences due to biomass burning. We use NOAA HYSPLIT back trajectories (https://www.ready.noaa.gov/hypub-bin/trajtype.pl?runtype=archive) overlaid on top of recent hot spots using MODIS or NOAA Hazard Mapping System Fire and Smoke Product (https://www.ospo.noaa.gov/Products/land/hms.html) to ascertain whether smoke and biomass burning influences are contributing to particular ozone enhancements observed in the profiles.

Figure 3 shows the back trajectories of air parcels with starting altitudes at the height of the ozone enhancement just above the boundary layer on the afternoon flight of 15 May 2017 from El Paso. The back trajectories show likely paths that the air parcels above El Paso at that time followed over the prior 96 hours. The back trajectories are overlaid on top of recent MODIS hot spots where the red dots show sites of possible biomass burning from the previous 24 hours and the yellow dots show the sites of possible biomass burning from the previous seven days. The ozone enhancement we see on 15 May 2017 may have had contributions resulting from long-range transport resulting from the influences of biomass burning emissions. The Appendix contains more information about the standard HYSPLIT trajectories that we calculate and guidelines about their range of applicability. The ozonesonde data and analysis suggest that this event could make a good case study for modeling to ascribe relative contributions of biomass burning and local production to the boundary layer ozone concentrations.

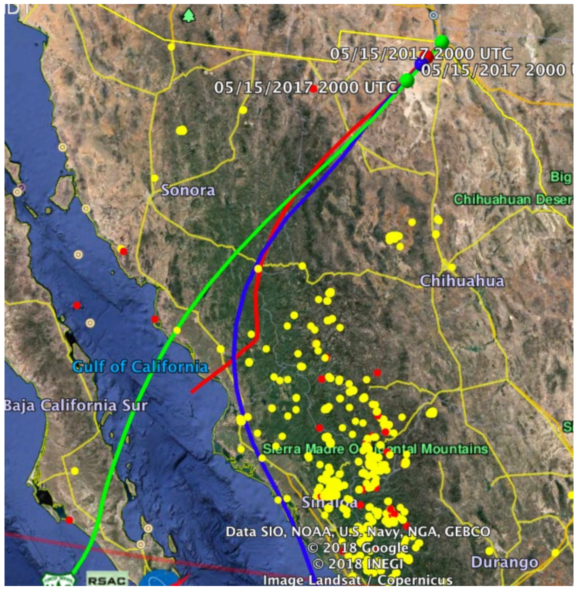

***Figure 3**. The profile of the sounding on 15 May 2017 (**Figure 2**) has an ozone enhancement in the LFT with a peak at 5500 m AMSL. The enhancement may have resulted from the long-range transport of biomass burning emissions. Left: HYSPLIT back trajectories at 3000 m (red), 4250 m (blue), and 5500 m (green) AMSL overlaid on recent MODIS hot spots (red and yellow dots).*

1.1.2. Stratosphere-Troposphere Exchange

The stratospheric ozone layer has ozone concentrations that are a couple of orders of magnitude greater than what is observed at the surface. After a cold front, a tropopause fold may result in stratospheric air (high in ozone) mixing down into the troposphere a process known as stratosphere-troposphere exchange (STE) (Reiter, 1975; Shapiro, 1980). Post-frontal conditions often consist of clear skies, dry air, and weak or stagnant winds, conditions conducive to local ozone formation (Ngan et al., 2012). Such conditions, typically found one to three days after a frontal passage, often correlate with high ozone days.

Stratospheric air is very dry, and thus a sign of potential STE is when there is an ozone enhancement that simultaneously has very dry air with relative humidity (RH) < 5% (Appenzeller & Davies, 1992). HYSPLIT back trajectories typically show some descent for the air contributing to such a feature (Langford et al., 2018). Further, for cases where the back trajectories pass over the Rocky Mountains, the mountain range may facilitate downward transport (Langford et al., 2009).

1.2. Identifying Contributions from the Residual Layer

During most flight days in the 2019 campaign there were twice-daily launches with one at dawn to capture the nocturnal boundary layer and residual layer, and the other in the afternoon near the time of peak surface ozone. **Figure 1** shows the profiles of two ozonesonde flights on 3 August 2019 from El Paso. The altitude on the vertical axis is km above mean sea level (AMSL). Profiles of the ozone are shown in light blue for the morning flight and dark blue for the afternoon flight. Profiles of relative humidity (RH) are shown in green for the morning flight and dark green for the afternoon flight. Potential temperature (θ) profiles are shown in red for the morning flight and dark red for the afternoon flight. The potential temperature is the temperature (in Kelvin) that a parcel of air would have if adiabatically transported to a standard pressure (i.e., 1000 hPa or surface pressure). The stability of the air can be determined by the vertical gradient (as a function of height z) of the potential temperature. The top of the afternoon boundary layer (BL) is marked by the black horizontal line. Just above the surface for the afternoon potential temperature profile, $\partial\theta/\partial z < 0$, which indicates the air is unstable (due to surface heating). After the initial negative gradient near the surface, the potential temperature is approximately constant ($\partial\theta/\partial z = 0$) to the top of the boundary layer near 3.9 km AMSL on this day. A near zero gradient in potential temperature is common. Above the boundary layer, the atmosphere is stable as indicated by the potential temperature gradient being positive ($\partial\theta/\partial z > 0$). The larger a positive potential temperature gradient is, the stronger the stability of the atmosphere at that altitude.

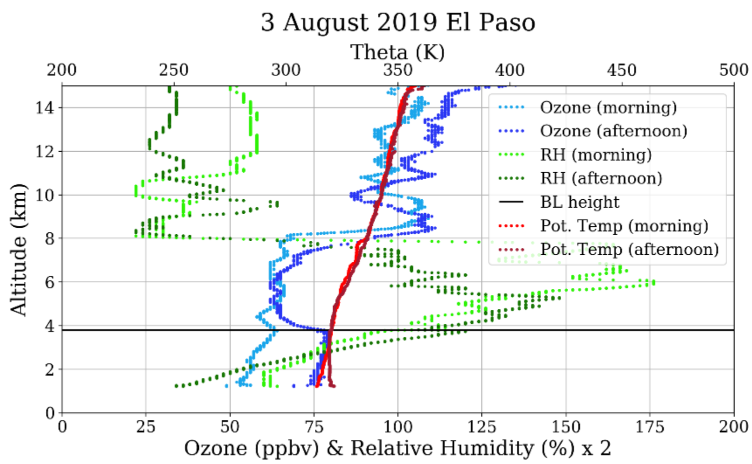

Figure 4. *For El Paso, the first day during the 2019 sampling period with an MDA8 ozone concentration in exceedance of the NAAQS ozone standard was 3 August. The image shows dawn (light blue and light green) and afternoon (dark blue and dark green) ozone and relative humidity profiles. The twice-daily profiles allow for estimates of the contribution of the residual layer from the previous night to the subsequent afternoon boundary layer ozone concentrations.*

Air in the morning residual layer will become entrained in the growing morning boundary layer, mixing into what becomes the afternoon boundary layer. Measurements of the morning residual layer ozone concentrations can provide an estimate of the starting point for production of the boundary layer ozone concentrations seen in the afternoon.

2. El Paso

There were 26 ozonesondes launched from the University of Texas at El Paso (UTEP) campus in El Paso. The typical pattern of two ozonesondes for each flight day included a morning ozonesonde at ~6 am LT (local time is UTC-6) and an afternoon ozonesonde at ~2 pm LT. **Table 1** shows profiles of ozone (blue), relative humidity (green), and potential temperature (red) for each ozonesonde launch from the UTEP campus in El Paso in 2023. On two days, 28 June and 6 July 2023, the afternoon ozonesonde was called off and there was only the morning ozonesonde on those days. There was a connection issue for the ozonesonde launched on the afternoon of 18 July, which resulted in no ozone data being recorded for that flight.

Table 1. *Ozonesonde profiles from El Paso in 2023. The profiles show the first 7 km above mean sea level (AMSL). The ozone (blue), relative humidity (green) and potential temperature (red) are shown. Morning profiles are shown on the left and afternoon profiles are shown on the right.*

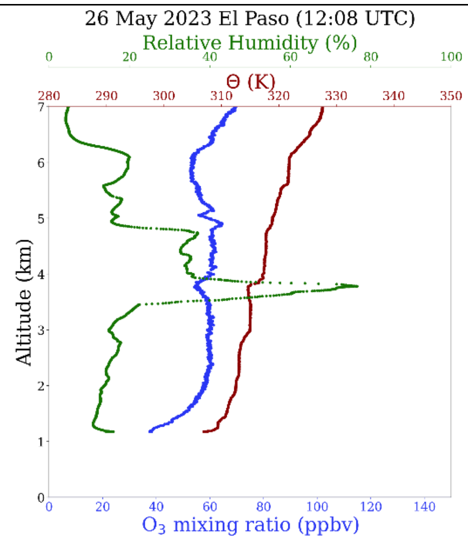

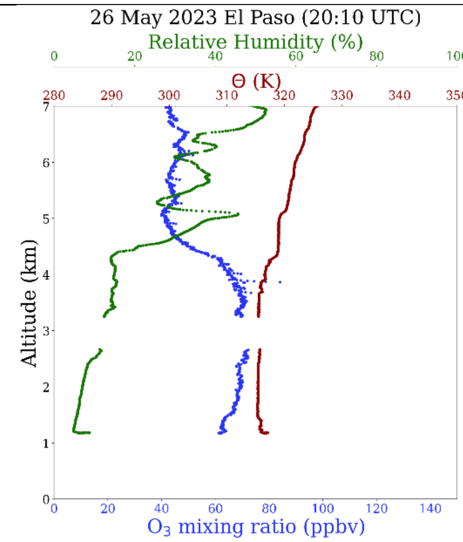

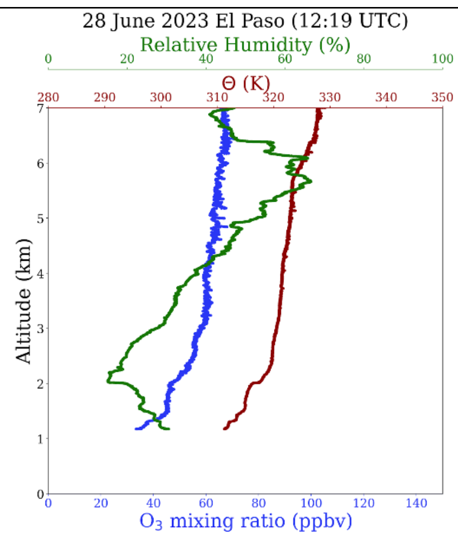

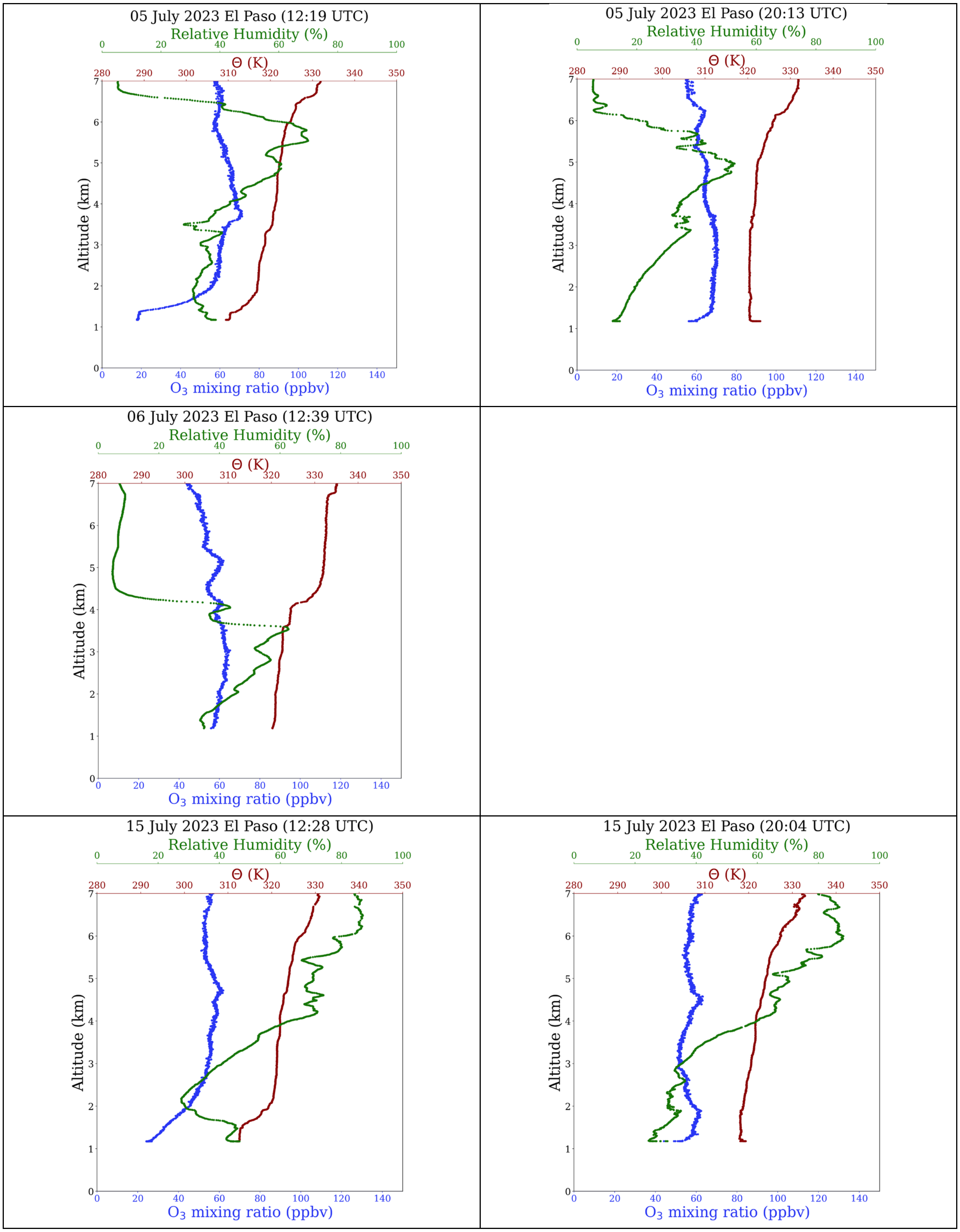
05 July 2023 El Paso (12:19 UTC)
Relative Humidity (%)
Θ (K)
Altitude (km)
O3 mixing ratio (ppbv)
05 July 2023 El Paso (20:13 UTC)
Relative Humidity (%)
Θ (K)
Altitude (km)
O3 mixing ratio (ppbv)
06 July 2023 El Paso (12:39 UTC)
Relative Humidity (%)
Θ (K)
Altitude (km)
O3 mixing ratio (ppbv)
15 July 2023 El Paso (12:28 UTC)
Relative Humidity (%)
Θ (K)
Altitude (km)
O3 mixing ratio (ppbv)
15 July 2023 El Paso (20:04 UTC)
Relative Humidity (%)
Θ (K)
Altitude (km)
O3 mixing ratio (ppbv)

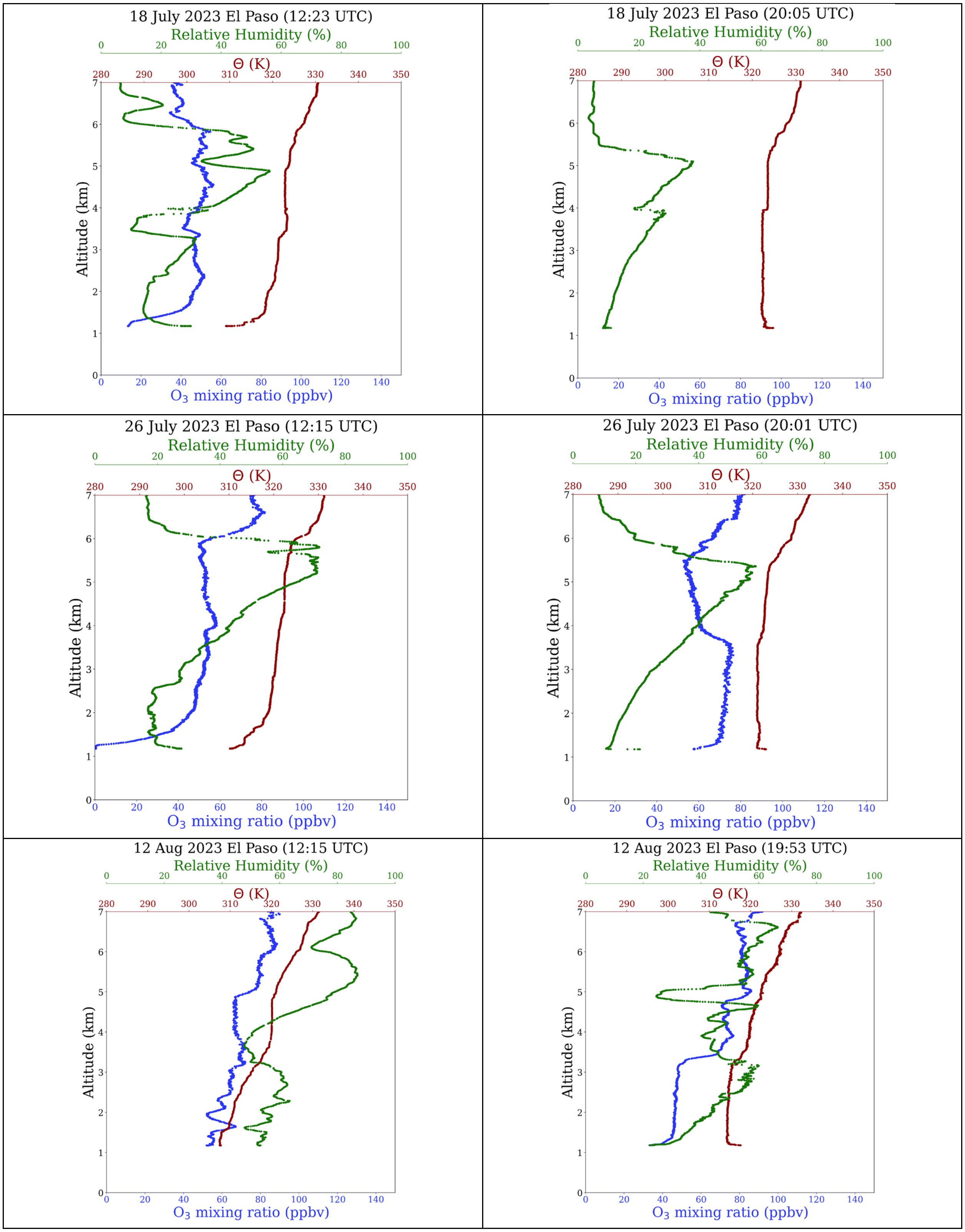
18 July 2023 El Paso (12:23 UTC)
18 July 2023 El Paso (20:05 UTC)
26 July 2023 El Paso (12:15 UTC)
26 July 2023 El Paso (20:01 UTC)
12 Aug 2023 El Paso (12:15 UTC)
12 Aug 2023 El Paso (19:53 UTC)
Relative Humidity (%)
Θ (K)
Altitude (km)
O3 mixing ratio (ppbv)

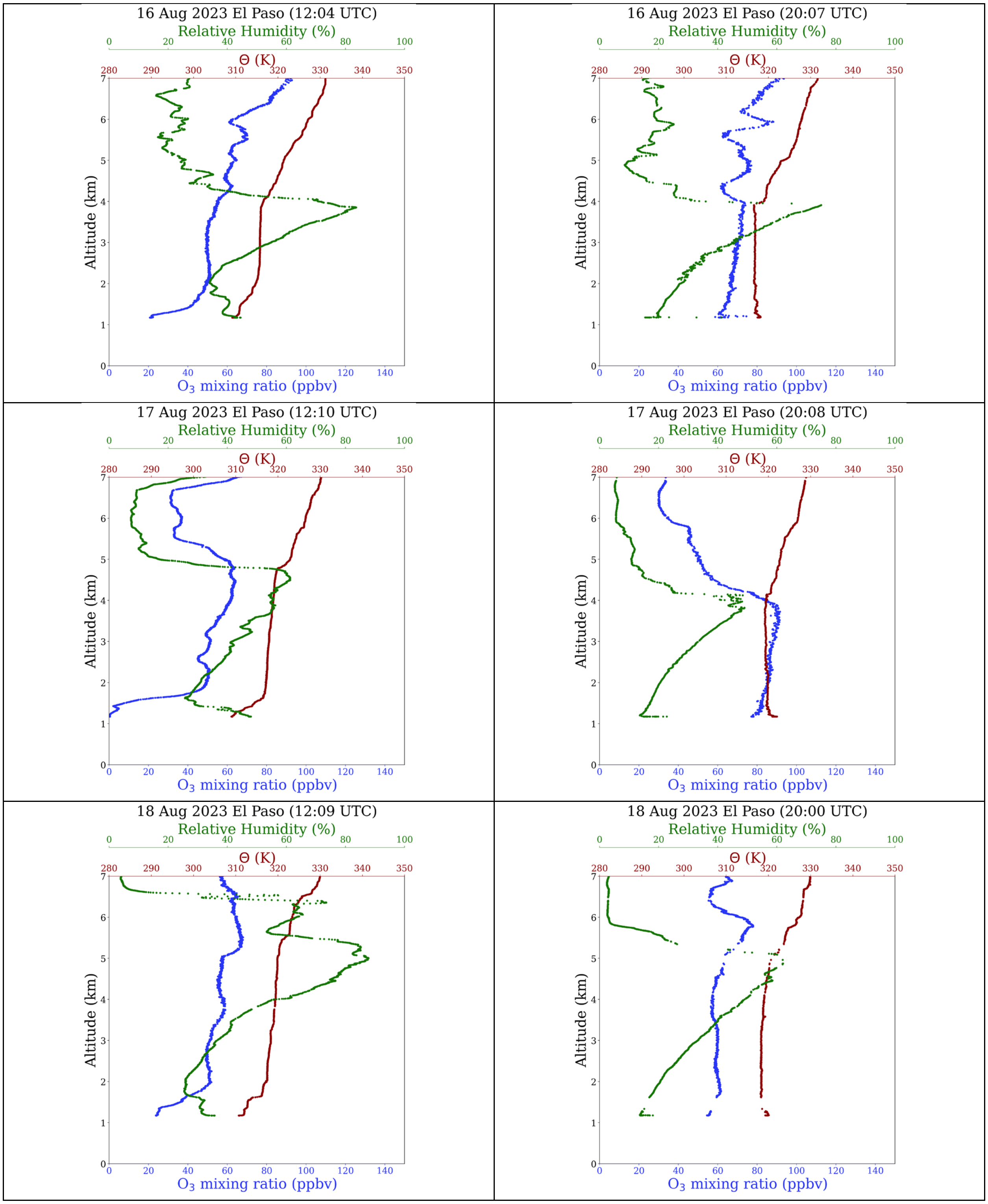
16 Aug 2023 El Paso (12:04 UTC)
16 Aug 2023 El Paso (20:07 UTC)
17 Aug 2023 El Paso (12:10 UTC)
17 Aug 2023 El Paso (20:08 UTC)
18 Aug 2023 El Paso (12:09 UTC)
18 Aug 2023 El Paso (20:00 UTC)
Relative Humidity (%)
Θ (K)
Altitude (km)
O_3 mixing ratio (ppbv)

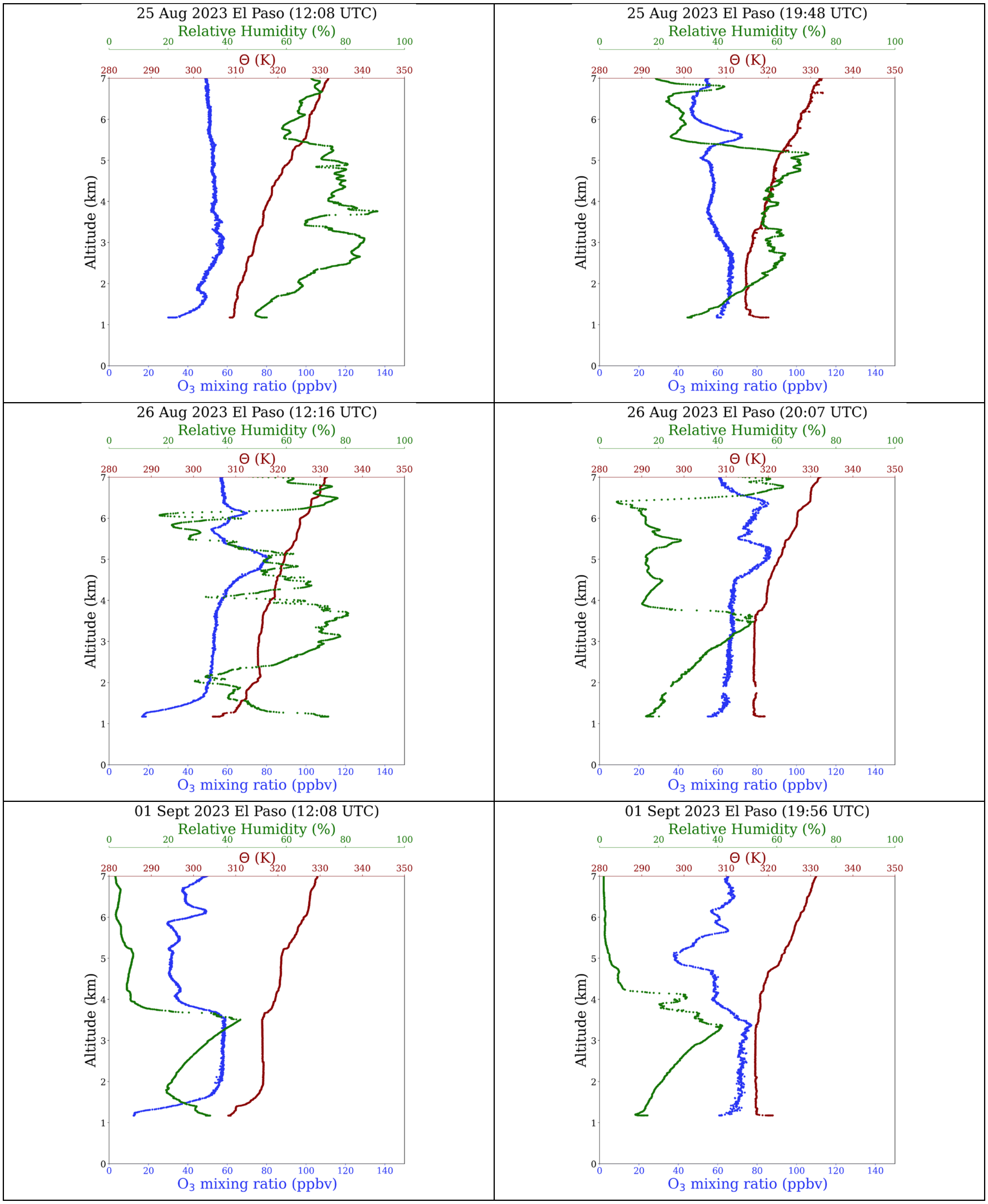

During the prior campaigns the C12 UTEP monitor (no longer active) recorded more exceedance events than the other CAMS locations in the region. Some of the ozonesonde profiles from this campaign reflect elevated ozone levels above the UTEP campus, such as the afternoon profile on August 17, which shows > 80 ppbv of ozone in the first three kilometers above the surface.

The new CAMS 1021 Ojo de Agua site (serves as C12 UTEP site) offers new opportunities to study air quality on the northwest side of El Paso to the west of the Franklin mountains. During the sampling period, there were seven days where the C1021 Ojo de Agua site exceeded the ozone standard: July 3, July 4, August 1, August 3, August 4, August 28, and August 31. **Figure 5** shows the 24-hour wind runs for the C1021 Ojo de Agua site for August 4 and August 31, the two highest ozone days for the El Paso region during the sampling period. The wind runs link together the hourly wind from a monitoring site, and the color scale shows the ozone for that specific hour. For both days, the ozone reached its maximum when winds had a southerly component, which could be an indication of influences from cross-border transport from Juarez.

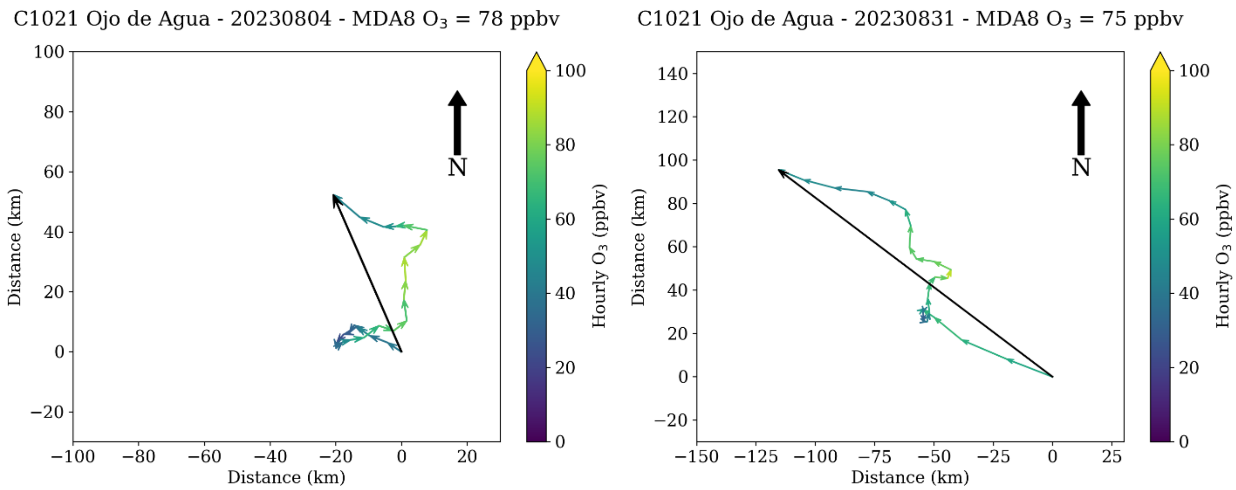

Figure 5. *24-hour wind runs for the C1021 Ojo de Agua monitor on August 4 (left) and August 31 (right), the two highest ozone days in the El Paso region during the sampling period.*

3. San Antonio

There were 24 ozonesondes launched from the Trinity University campus in San Antonio from 25 August – 17 October 2023. The typical sampling strategy was for one ozonesonde launch in the morning and another in the afternoon. Restrictions on weekdays were such that the first ozonesonde was launched at 7 am LT and the second was launched after 5 pm LT (local time is UTC-5). **Table 2** shows profiles of ozone (blue), relative humidity (green), and potential temperature (red) for each ozonesonde launch from the Trinity University campus in San Antonio in 2023. During the campaign, a couple of flights had issues collecting data. On September 1, no ozone data was collected. On September 27, the planned afternoon launch was scrubbed due to rain and so there was only one flight on that day. On another day, September 28, there was an afternoon ozonesonde launch, however, due to an issue with the receiving system (which was later corrected), no data from that flight was collected.

Table 2. *Ozonesonde profiles from San Antonio in 2023. The profiles show the first 7 km above mean sea level (AMSL). The ozone (blue), relative humidity (green) and potential temperature (red) are shown. Morning profiles are shown on the left and afternoon profiles are shown on the right.*

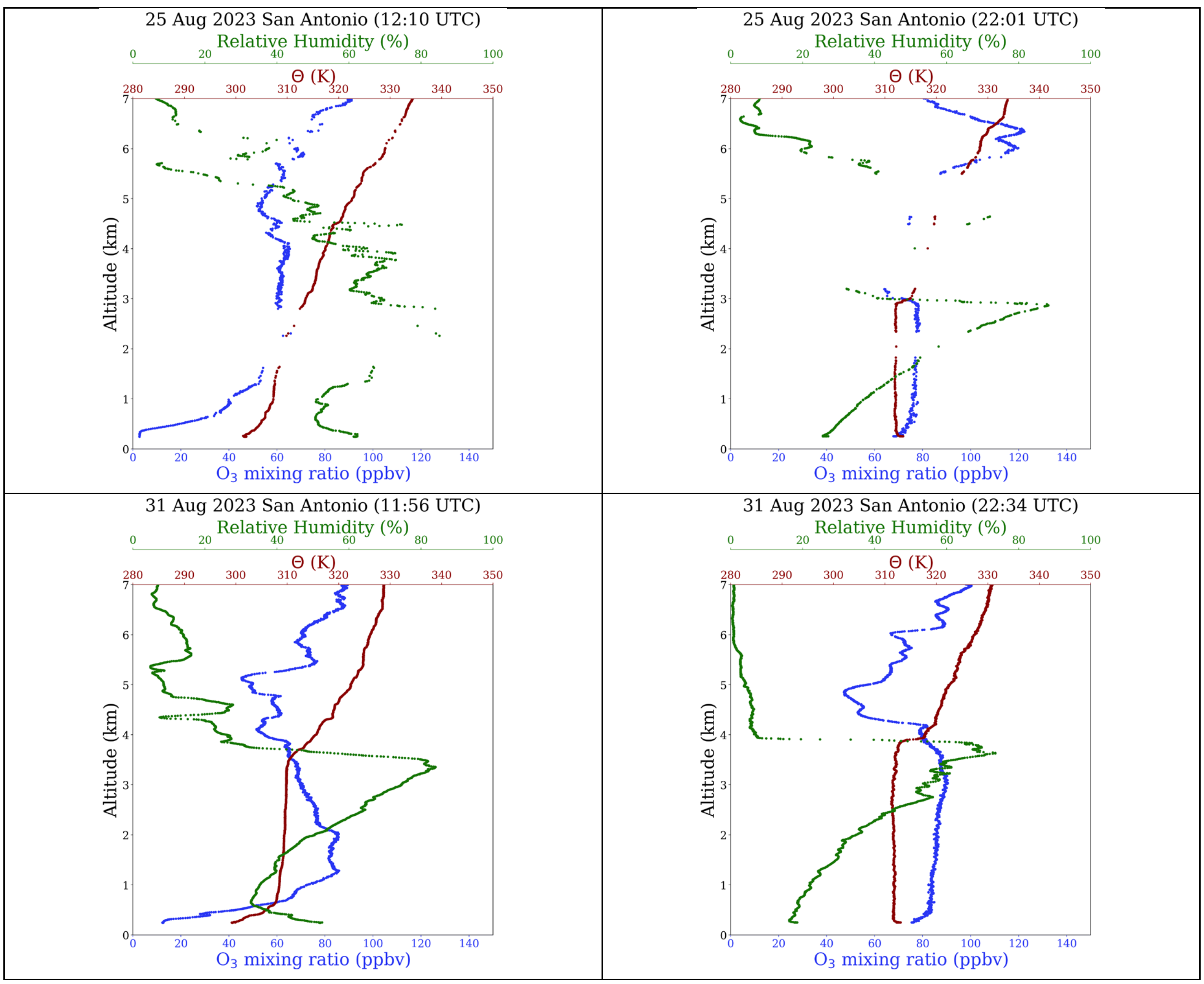

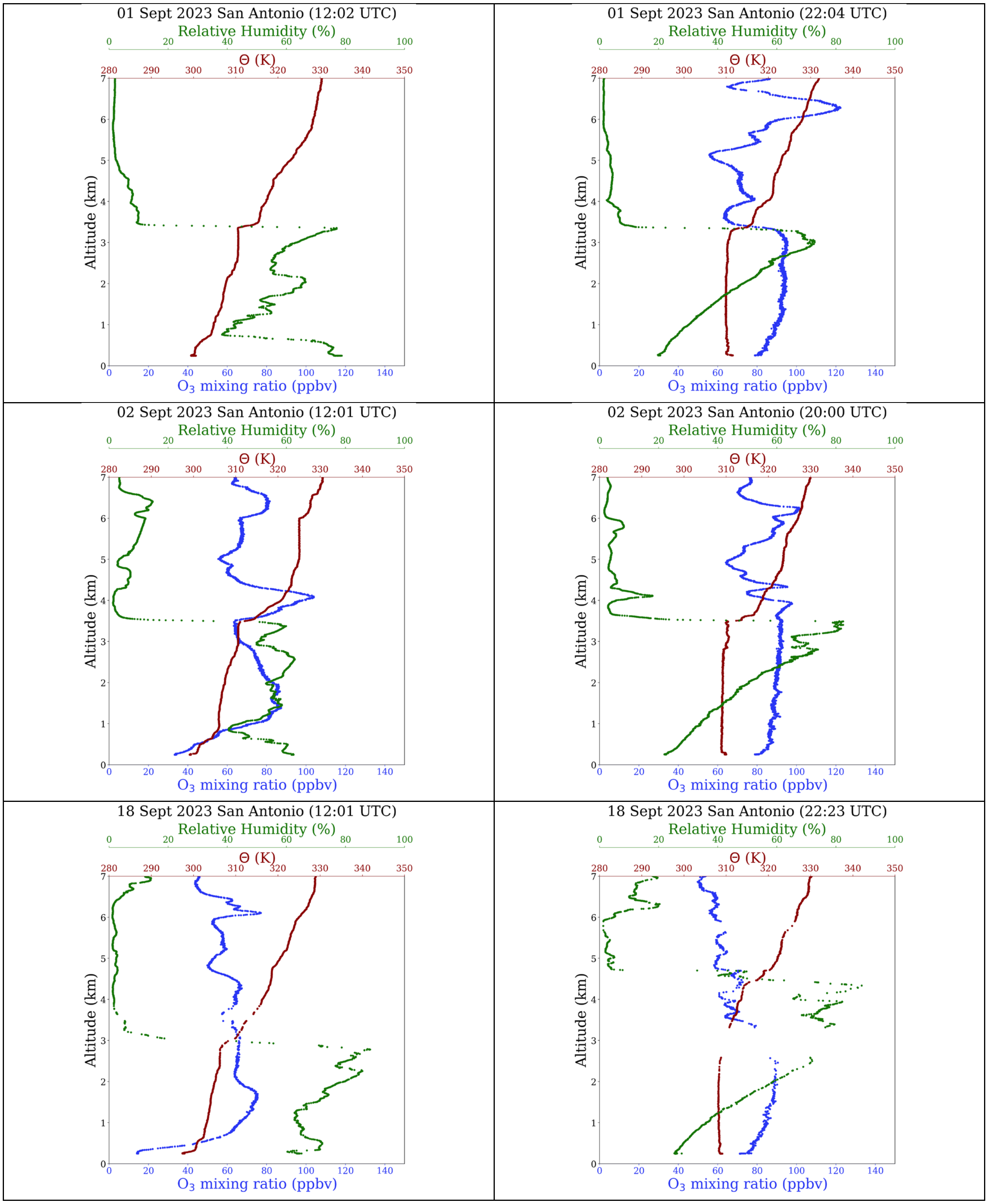
01 Sept 2023 San Antonio (12:02 UTC)
01 Sept 2023 San Antonio (22:04 UTC)
02 Sept 2023 San Antonio (12:01 UTC)
02 Sept 2023 San Antonio (20:00 UTC)
18 Sept 2023 San Antonio (12:01 UTC)
18 Sept 2023 San Antonio (22:23 UTC)
Relative Humidity (%)
Θ (K)
Altitude (km)
O3 mixing ratio (ppbv)

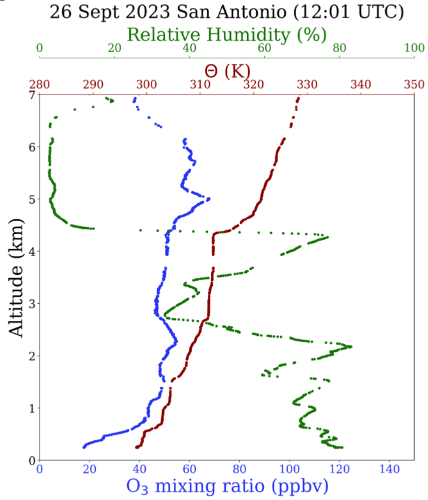
26 Sept 2023 San Antonio (12:01 UTC)
Relative Humidity (%)
Θ (K)
Altitude (km)
O3 mixing ratio (ppbv)

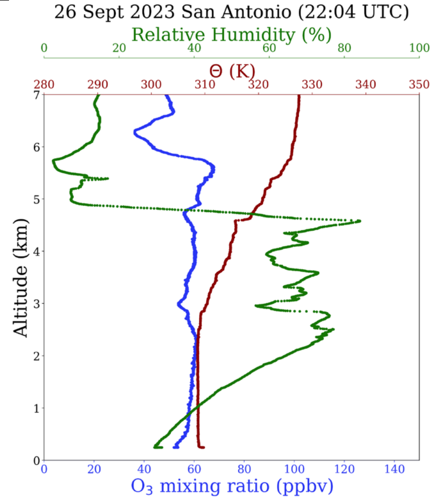
26 Sept 2023 San Antonio (22:04 UTC)
Relative Humidity (%)
Θ (K)
Altitude (km)
O3 mixing ratio (ppbv)

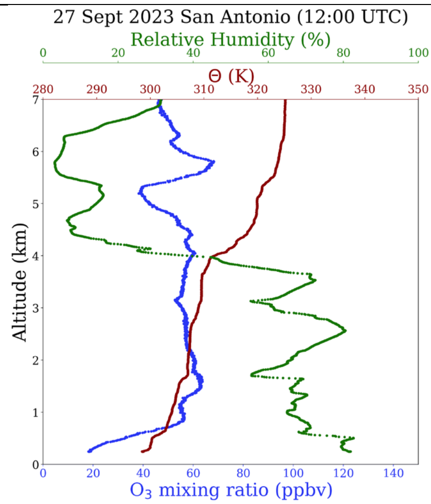
27 Sept 2023 San Antonio (12:00 UTC)
Relative Humidity (%)
Θ (K)
Altitude (km)
O3 mixing ratio (ppbv)

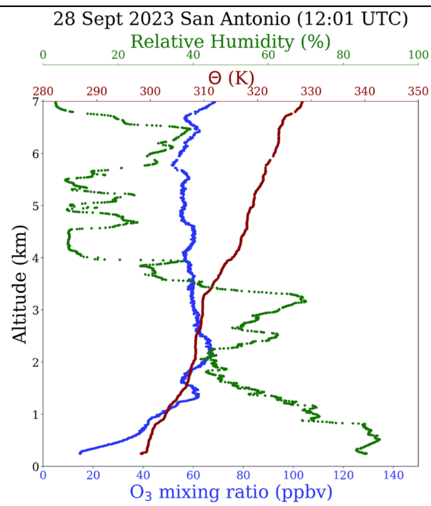
28 Sept 2023 San Antonio (12:01 UTC)
Relative Humidity (%)
Θ (K)
Altitude (km)
O3 mixing ratio (ppbv)

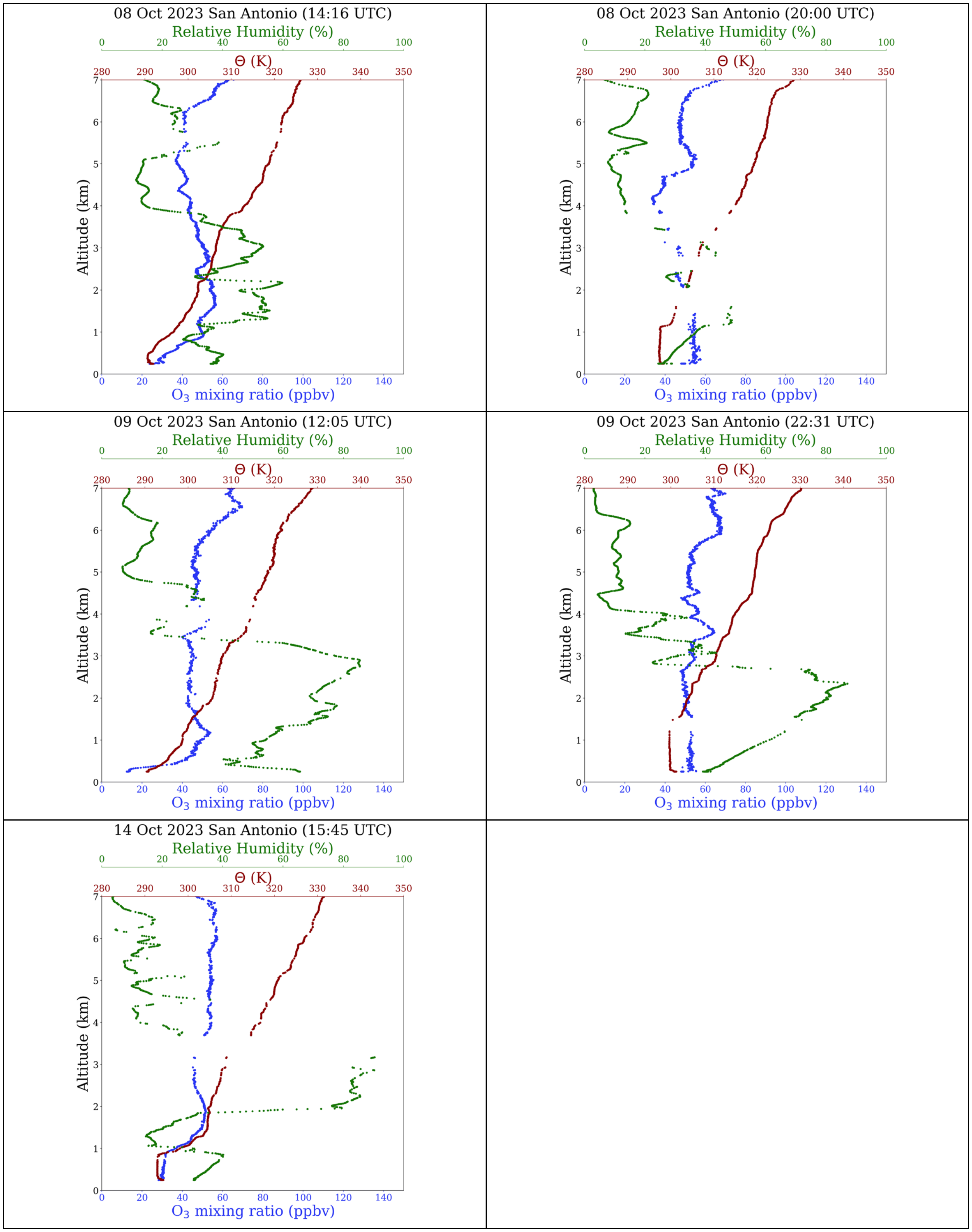
08 Oct 2023 San Antonio (14:16 UTC)
08 Oct 2023 San Antonio (20:00 UTC)
09 Oct 2023 San Antonio (12:05 UTC)
09 Oct 2023 San Antonio (22:31 UTC)
14 Oct 2023 San Antonio (15:45 UTC)
Relative Humidity (%)
Θ (K)
Altitude (km)
O3 mixing ratio (ppbv)

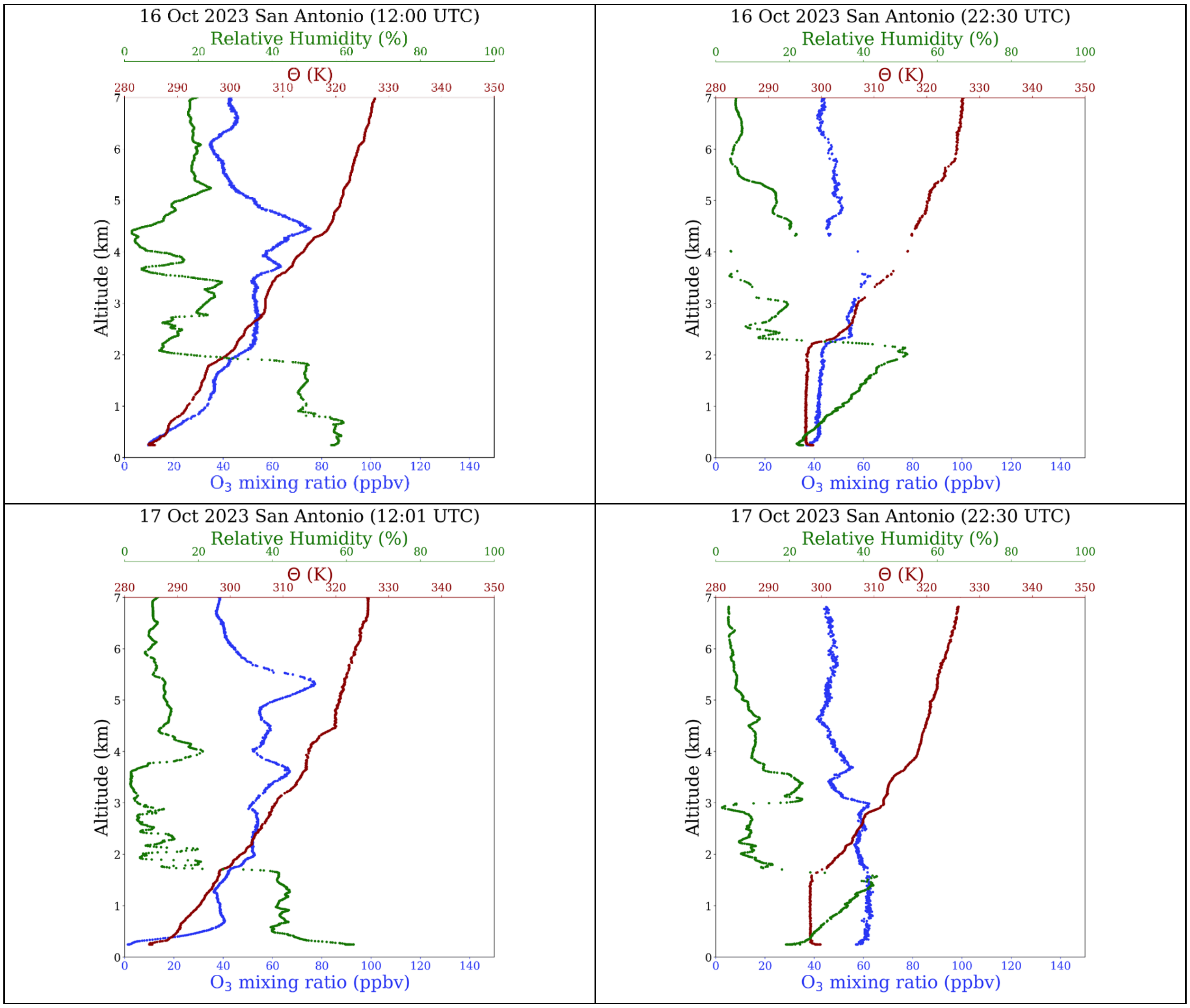

During the sampling period of 25 August – 17 October 2023, there were 13 days where one of the CAMS in the San Antonio region exceeded the MDA8 ozone standard. Ozonesondes were launched on six of those days: August 25, August 31, September 1, September 2, September 18, and September 27. The morning ozonesondes capture how near-surface ozone is close to zero while aloft there is ozone left over in the nocturnal residual layer. As the boundary layer grows throughout the day, the convection resulting from surface heating mixes in some of the residual layer. On days exceeding the ozone standard, residual layer ozone left over from the day before often has a significant contribution. **Table 3** shows the peak value of O3 in the residual layer identified from the morning ozonesonde profile and the peak O3 in the afternoon boundary layer identified from the afternoon ozonesonde profile for days that exceeded the ozone standard and ozonesondes were launched.

Table 3. *For days that exceeded the MDA8 ozone standard in the San Antonio region and ozonesondes were launched, the table shows the potential contribution of ozone in the residual layer that later mixed into the boundary layer as it developed throughout the day. Also shown is the monitor in the San Antonio region that recorded the highest MDA8 O3.*

Date	**Peak Residual Layer O3 (ppbv)**	**Peak Afternoon Boundary Layer O3 (ppbv)**	**Highest MDA8 O3 (ppbv)**	**CAMS (for highest MDA8 O3)**
8/25/2023	60	75	73	C622 Heritage Middle School
8/31/2023	85	85	82	C622 Heritage Middle School
9/1/2023	N/A	90	81	C58 Camp Bullis
9/2/2023	85	90	76	C58 Camp Bullis
9/18/2023	75	90	74	C23 San Antonio Northwest & C58
9/27/2023	60	N/A	77	C505 Garden Ridge

The ozone exceedance days in the San Antonio region were often in post-frontal conditions. On August 31 and September 1, there was a stationary front along the Gulf coast that led to clear skies and slack winds in the San Antonio region during that ozone episode. Wind speeds were particularly low overnight leading to the residual layer air aloft of San Antonio to remain in the area. The ozone exceedance day on September 18 was in post-frontal conditions. San Antonio was at the center of a high pressure system on September 27 with a cold front passing through before.

The left column of **Table 4** shows 24-hour wind runs (each hourly wind vector connected together) for the CAMS with the highest MDA8 O3 for each of the six exceedance days in which ozonesondes were launched. The right column of Table 4 shows the 72-hour HYSPLIT back trajectories of air masses that contributed to the afternoon boundary layer in San Antonio.

Table 4. *24-hour wind runs (left) and 72-hour HYSPLIT back trajectories (right) for each ozone exceedance day in the San Antonio region for which ozonesondes were launched.*

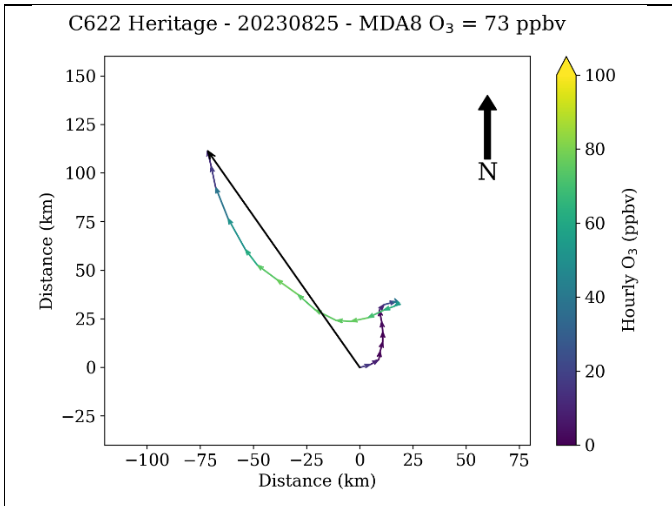

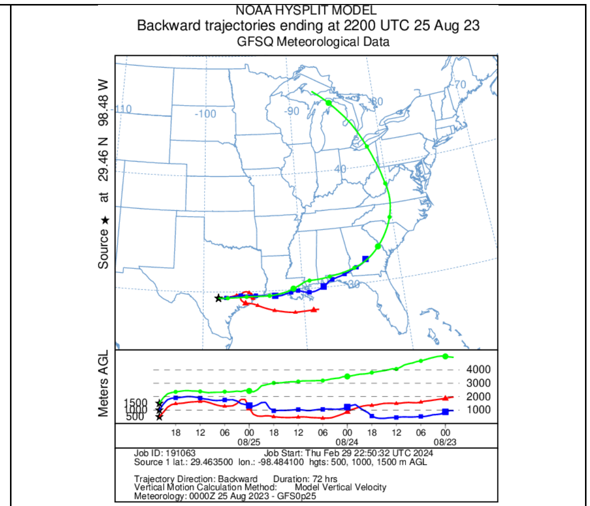

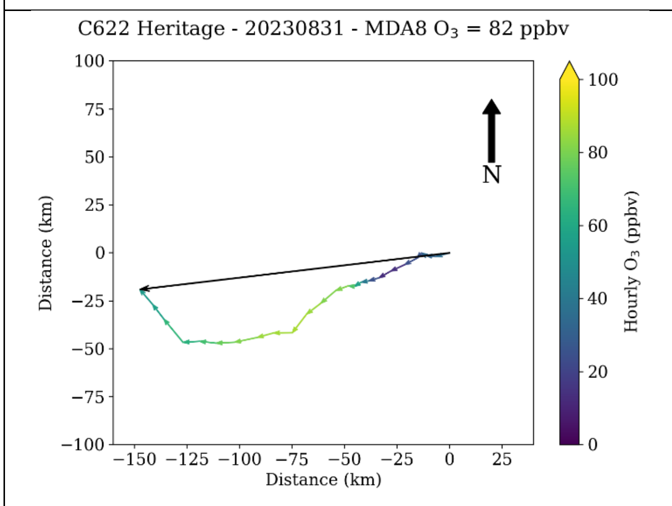

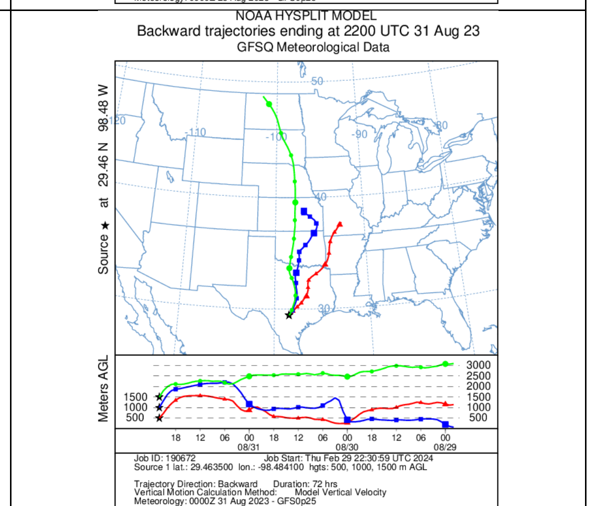

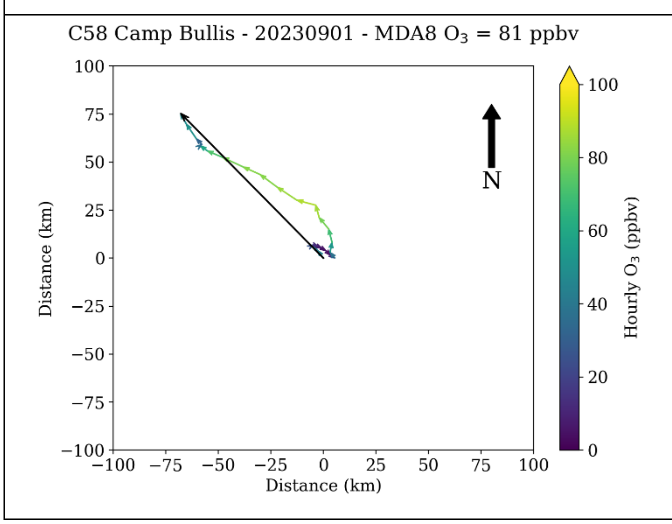

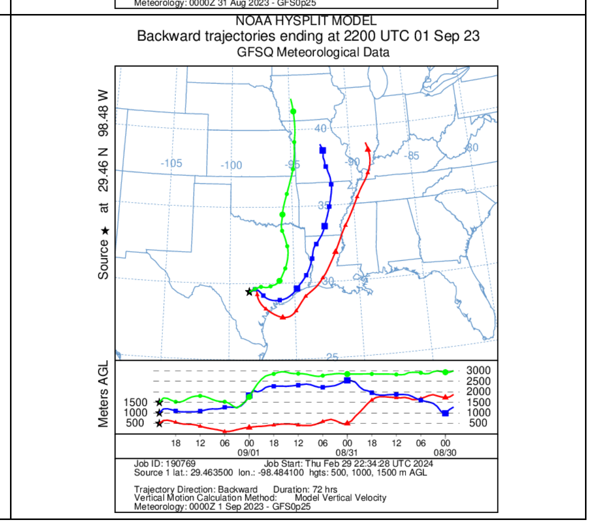

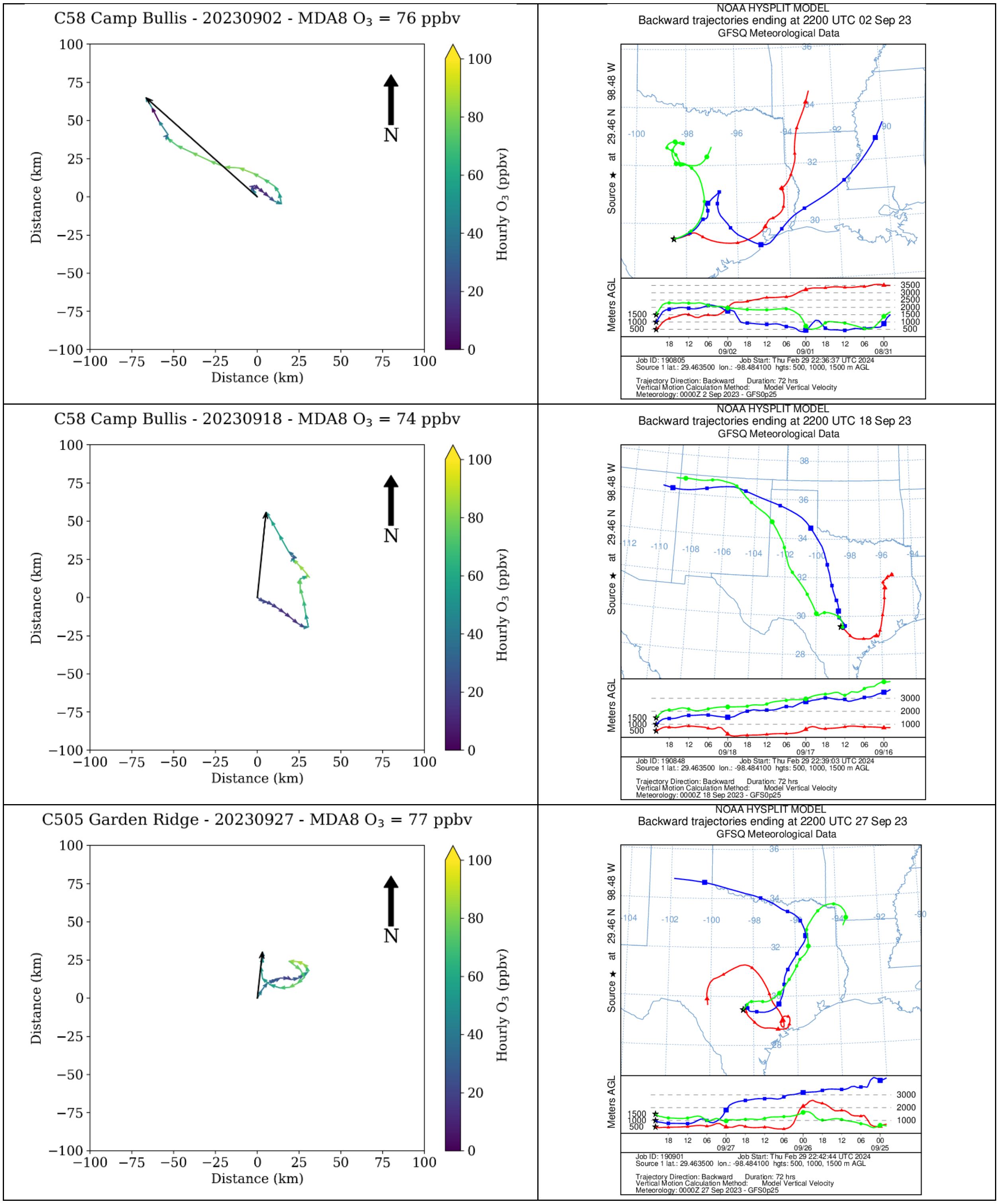

4. Houston

There were ten ozonesondes launched from the Houston-Galveston-Brazoria (HGB) region as part of this project in September 2023. Another 24 ozonesondes were launched from the HGB region as part of a separately funded TCEQ project. Of the ten ozonesondes allotted for this project, eight were from the University of Houston Energy Research Park and two were from the University of Houston Coastal Center. **Table 3** shows profiles of ozone (blue), relative humidity (green), and potential temperature (red) for each ozonesonde launch from the HGB region in September 2023. Morning ozonesonde profiles are in the left column and afternoon ozonesondes are in the right column. The sampling period for ozonesonde data collection in the HGB region began and concluded in the month of September.

Table 5. *Ozonesonde profiles from Houston in 2023 that were a part of this project. The profiles show the first 7 km above mean sea level (AMSL). The ozone (blue), relative humidity (green) and potential temperature (red) are shown.*

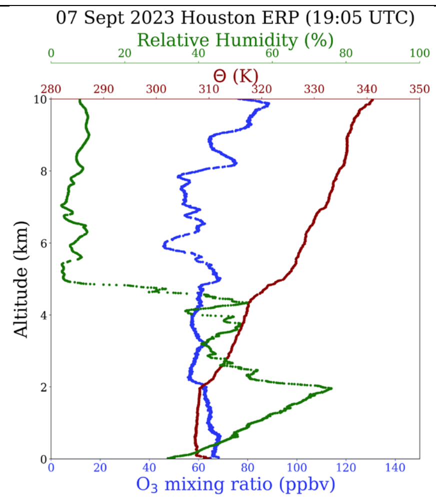

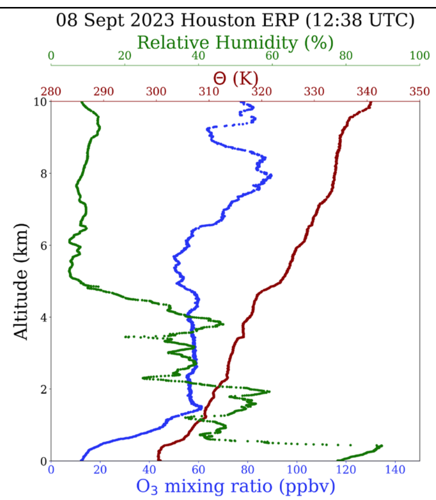

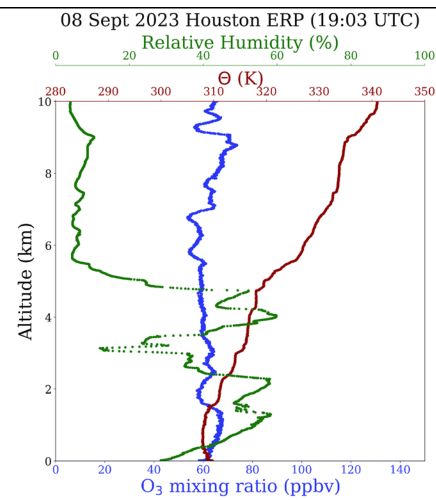

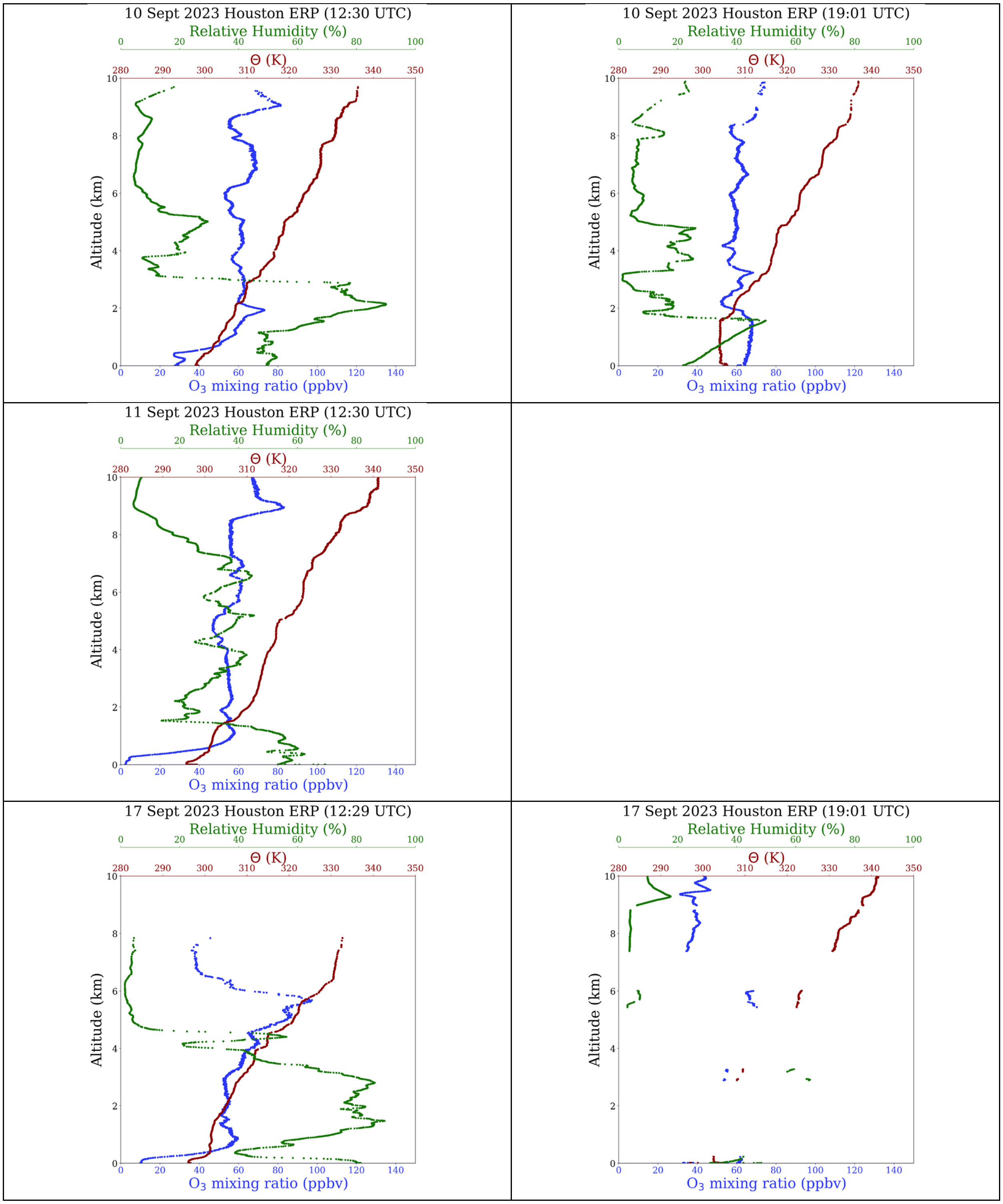
10 Sept 2023 Houston ERP (12:30 UTC)
Relative Humidity (%)
Θ (K)
Altitude (km)
O_3 mixing ratio (ppbv)
10 Sept 2023 Houston ERP (19:01 UTC)
Relative Humidity (%)
Θ (K)
Altitude (km)
O_3 mixing ratio (ppbv)
11 Sept 2023 Houston ERP (12:30 UTC)
Relative Humidity (%)
Θ (K)
Altitude (km)
O_3 mixing ratio (ppbv)
17 Sept 2023 Houston ERP (12:29 UTC)
Relative Humidity (%)
Θ (K)
Altitude (km)
O_3 mixing ratio (ppbv)
17 Sept 2023 Houston ERP (19:01 UTC)
Relative Humidity (%)
Θ (K)
Altitude (km)
O_3 mixing ratio (ppbv)

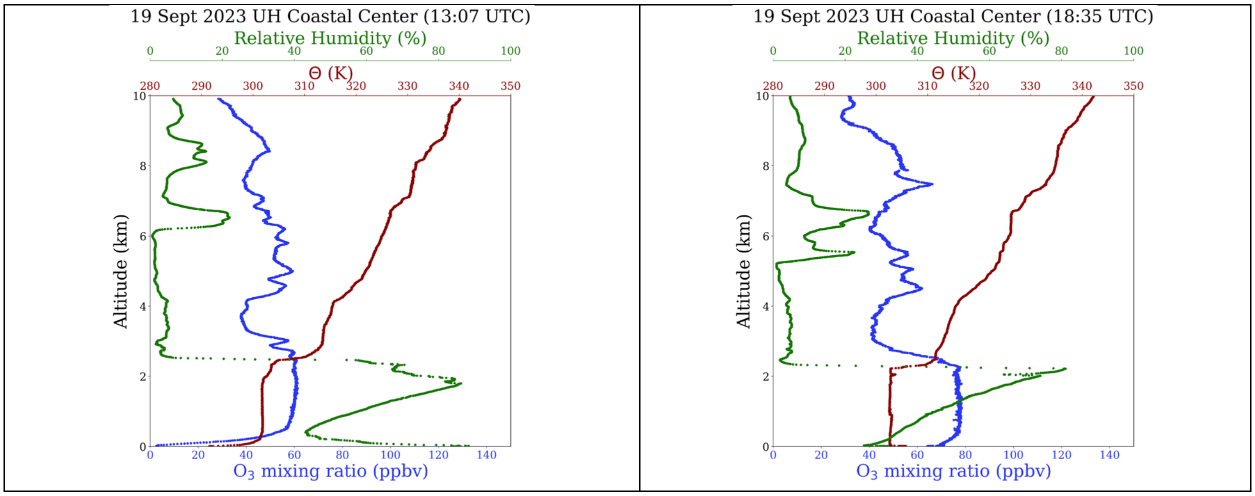

Table 6 shows the peak value of O3 in the residual layer identified from the morning ozonesonde profile and the peak O3 in the afternoon boundary layer identified from the afternoon ozonesonde profile for days that exceeded the ozone standard and ozonesondes were launched from the HGB region as part of this project.

Table 6. *For days that exceeded the MDA8 ozone standard in the San Antonio region and ozonesondes were launched, the table shows the potential contribution of ozone in the residual layer that later mixed into the boundary layer as it developed throughout the day. Also shown is the monitor in the San Antonio region that recorded the highest MDA8 O3.*

Date	Peak Residual Layer O3 (ppbv)	Peak Afternoon Boundary Layer O3 (ppbv)	Highest MDA8 O3 (ppbv)	CAMS (for highest MDA8 O3)
9/10/2023	60	65	76	C1034 Galveston 99th St
9/11/2023	55	N/A	97	C53 Bayland Park
9/17/2023	55	N/A	83	C1034 Galveston 99th St
9/19/2023	60	75	89	C26 Northwest Harris Co.

On September 10 there was a stationary front off the coast in the Gulf of Mexico, and that stationary front was over the HGB region on September 11. September 17 was in post-frontal conditions. On September 19, a high pressure was in place over central and southeastern Texas.

The left column of **Table 7** shows 24-hour wind runs (each hourly wind vector connected together) for the CAMS with the highest MDA8 O3 for each of the four exceedance days in which ozonesondes were launched. The right column of Table 4 shows the 72-hour HYSPLIT back trajectories of airmasses that contributed to the afternoon boundary layer in Houston.

Table 7. *24-hour wind runs (left) and 72-hour HYSPLIT back trajectories (right) for each ozone exceedance day in the Houston-Galveston-Brazoria region for which ozonesondes were launched as part of this project.*

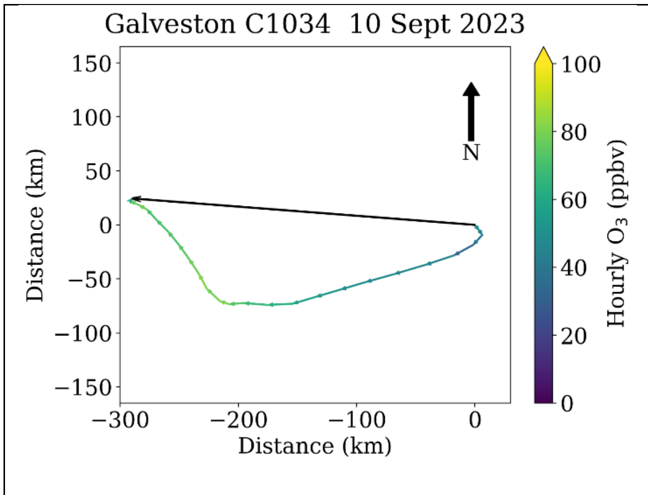

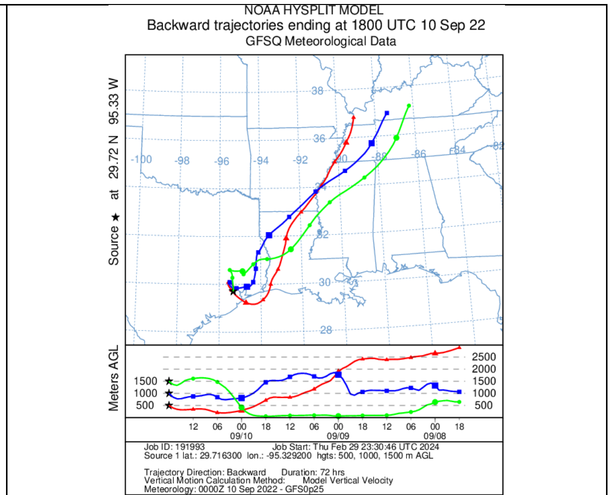

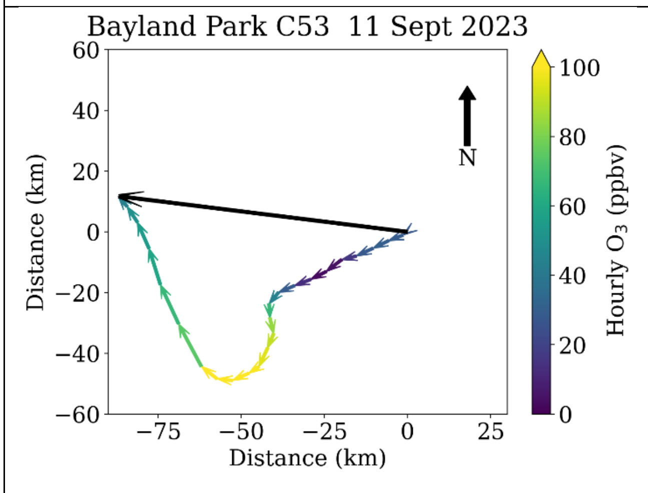

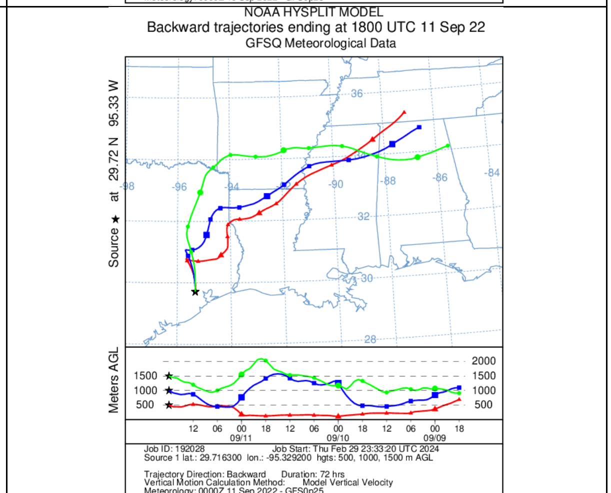

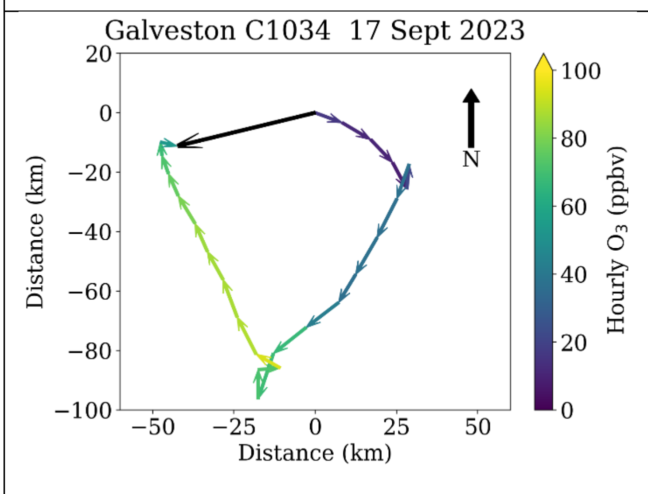

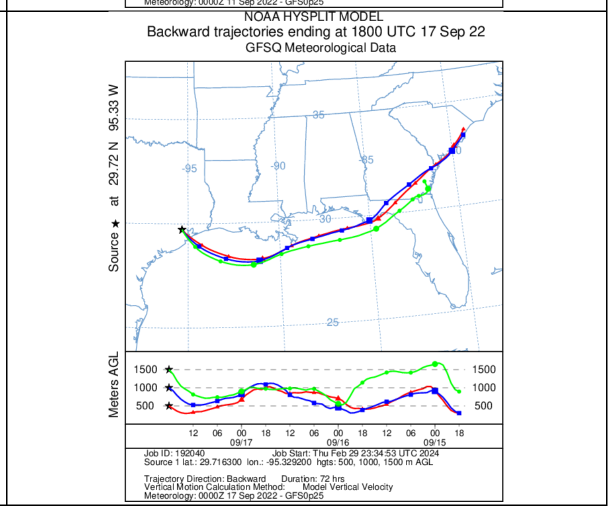

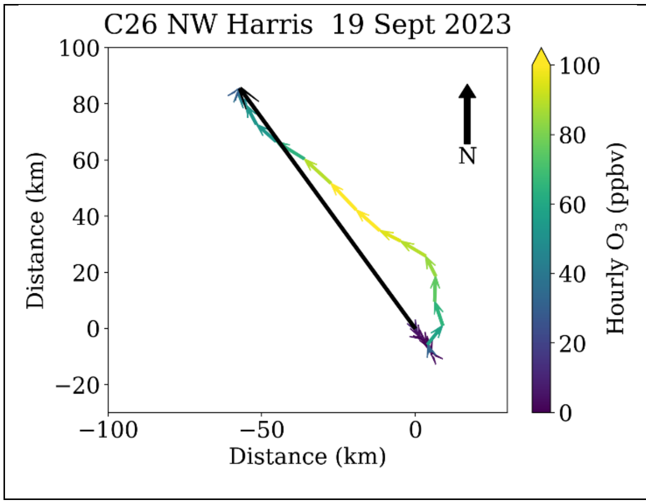
C26 NW Harris 19 Sept 2023
Distance (km)
Distance (km)
Hourly O_3 (ppbv)
N

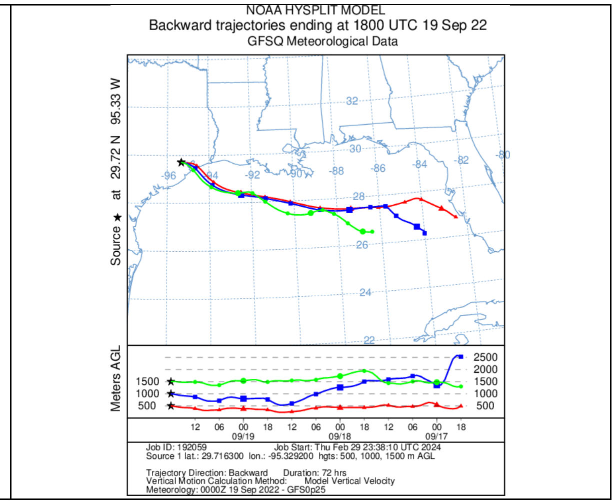
NOAA HYSPLIT MODEL
Backward trajectories ending at 1800 UTC 19 Sep 22
GFSQ Meteorological Data
Source ★ at 29.72 N 95.33 W
Meters AGL
Job ID: 192059 Job Start: Thu Feb 29 23:38:10 UTC 2024
Source 1 lat.: 29.716300 lon.: -95.329200 hgts: 500, 1000, 1500 m AGL
Trajectory Direction: Backward Duration: 72 hrs
Vertical Motion Calculation Method: Model Vertical Velocity
Meteorology: 0000Z 19 Sep 2022 - GFS0p25

5. Conclusions

For the days during the 2019 and 2020 campaigns that exceeded the ozone standard, there were signs of possible transport of ozone and its precursors into either the El Paso or Socorro, TX areas. Juarez was usually upwind of the high ozone areas observed in El Paso or Socorro, TX. When Juarez was upwind, slow steady winds may lead to an increase greater than 10 ppbv to the MDA8 ozone concentration on those days, and thus influence whether the El Paso and Socorro, TX monitors are in compliance with the NAAQS ozone standard. During the sampling period in 2023, there were seven days where the C1021 Ojo de Agua monitor exceeded the ozone standard, and the monitor was the highest monitor in the region on all but one of those days. On the two highest ozone days, ozone concentrations at the C1021 Ojo de Agua monitor were highest when the monitor recorded winds out of the south. Given its location in northwestern El Paso to the west of the Franklin Mountains, this result is consistent with findings of other monitors in the region where impacts of transport from Juarez may play a role. When conditions are favorable for ozone production, the transport of ozone and its precursors (e.g., NOx) into the El Paso area can lead to increases in ozone concentrations at key monitors that are in the path of the transported plume.

In San Antonio, post-frontal environments are very effective in creating conditions for high local ozone production, particularly when the return to southerly flow of moist, cleaner air from the Gulf of Mexico does not happen quickly. The plume affecting Camp Bullis and San Antonio Northwest monitors contains both elevated background ozone from continental transport and local ozone production from San Antonio. Recirculation of this combined air mass over San Antonio brings the polluted air back over the northwestern San Antonio monitors during the afternoon of a high ozone day. The dawn launches provide ozone profiles of the residual layer that can contribute to that day's afternoon peak ozone in the boundary layer as mixing occurs throughout the morning. For the days during the 2023 campaign that exceeded the ozone standard and had ozonesonde launches, the winds were typically slow overnight and during the day, enhancing the contributions of air from the previous day adding to the ozone found in the residual layer. The high background ozone present in the residual layer accelerated and enhanced local production resulting in exceedance days. As might be expected, the atmosphere was relatively clear of clouds and moisture on exceedance days.

In the Houston-Galveston-Brazoria region, there were ten ozonesondes launched as part of this project. The exceedance days observed in the HGB region spanned a range of conditions. In some cases, there were clear signs of the impacts of recirculating air masses resulting from bay and sea breezes impacting Houston and coastal (e.g., Galveston) sites.

There is limited evidence of stratospheric influence, due to low humidity and high ozone present above the boundary layer, but it is not clear that the stratospheric air is reaching the boundary layer. More work is needed to better quantify the potential impacts of transported ozone on boundary layer concentrations. This could potentially be done by incorporating modeling along with sonde profile analysis.

5.1. Opportunities for Future Work

On August 1, 2023, the NASA Tropospheric Emissions: Monitoring of Pollution (TEMPO) instrument on a satellite started taking measurements that will provide hourly scans over Texas. After it becomes available starting in April 2024, the satellite data will improve our ability to characterize ozone episodes in Texas and the ozonesondes from this project will offer a way of assessing TEMPO's performance and reliability of its data ozone data products across Texas, particularly in the boundary layer and lower free troposphere.

We also recommend that TCEQ or other entities continue to fund regular atmospheric sampling with ozonesondes during ozone seasons in these target areas, as well as other areas of interest, such as Dallas-Fort Worth, Austin-Round Rock, and others. Data from these campaigns contribute to continuous improvements in photochemical modeling, assessments of transport, and improve understanding of atmospheric conditions during high ozone events.

6. References

Appenzeller, C., & Davies, H. C. (1992). Structure of stratospheric intrusions into the troposphere. *Nature*, *358*(6387), Article 6387. https://doi.org/10.1038/358570a0

Jensen, M. P., Flynn, J. H., Judd, L. M., Kollias, P., Kuang, C., Mcfarquhar, G., Nadkarni, R., Powers, H., & Sullivan, J. (2022). A Succession of Cloud, Precipitation, Aerosol, and Air Quality Field Experiments in the Coastal Urban Environment. *Bulletin of the American Meteorological Society*, *103*(2), 103–105. https://doi.org/10.1175/BAMS-D-21-0104.1

Judd, L. M., Investigator, T.-A. C.-P., Sullivan, J. T., Investigator, T.-A. C.-P., Lefer, B., Haynes, J., Jensen, M. P., & Nadkarni, R. (2021). *TRACER-AQ Science Plan: An Interagency Cooperative Air Quality Field Study in the Houston, TX Metropolitan Region*. https://www-air.larc.nasa.gov/missions/tracer-aq/docs/TRACERAQ_SciencePlan_v1.pdf

Langford, A. O., Aikin, K. C., Eubank, C. S., & Williams, E. J. (2009). Stratospheric contribution to high surface ozone in Colorado during springtime. *Geophysical Research Letters*, *36*(12). https://doi.org/10.1029/2009GL038367

Langford, A. O., Alvarez, R. J., Brioude, J., Evan, S., Iraci, L. T., Kirgis, G., Kuang, S., Leblanc, T., Newchurch, M. J., Pierce, R. B., Senff, C. J., & Yates, E. L. (2018). Coordinated profiling of stratospheric intrusions and transported pollution by the Tropospheric Ozone Lidar Network (TOLNet) and NASA Alpha Jet experiment (AJAX): Observations and comparison to HYSPLIT, RAQMS, and FLEXPART. *Atmospheric Environment*, *174*, 1–14. https://doi.org/10.1016/j.atmosenv.2017.11.031

Ngan, F., Byun, D., Kim, H., Lee, D., Rappenglück, B., & Pour-Biazar, A. (2012). Performance assessment of retrospective meteorological inputs for use in air quality modeling during

TexAQS 2006. *Atmospheric Environment*, *54*, 86–96. https://doi.org/10.1016/j.atmosenv.2012.01.035

Reiter, E. R. (1975). Stratospheric-tropospheric exchange processes. *Reviews of Geophysics*, *13*(4), 459–474. https://doi.org/10.1029/RG013i004p00459

Shapiro, M. A. (1980). Turbulent Mixing within Tropopause Folds as a Mechanism for the Exchange of Chemical Constituents between the Stratosphere and Troposphere. *Journal of the Atmospheric Sciences*, *37*(5), 994–1004. https://doi.org/10.1175/1520-0469(1980)037<0994:TMWTFA>2.0.CO;2